

Effective Message Hiding with Order-Preserving Mechanisms

Gao Yu¹ Qiu Xuchong^{1*} Ye Zihan²

¹Bosch Corporate Research

²Xi'an Jiaotong-Liverpool University

{yu.gao2, xuchong.qiu}@cn.bosch.com, Zihan.Ye22@student.xjtlu.edu.cn

Abstract

Message hiding, a technique that conceals secret message bits within a cover image, aims to achieve an optimal balance among message capacity, recovery accuracy, and imperceptibility. While convolutional neural networks have notably improved message capacity and imperceptibility, achieving high recovery accuracy remains challenging. This challenge arises because convolutional operations struggle to preserve the sequential order of message bits and effectively address the discrepancy between these two modalities. To address this, we propose StegaFormer, an innovative MLP-based framework designed to preserve bit order and enable global fusion between modalities. Specifically, StegaFormer incorporates three crucial components: Order-Preserving Message Encoder (OPME), Decoder (OPMD) and Global Message-Image Fusion (GMIF). OPME and OPMD aim to preserve the order of message bits by segmenting the entire sequence into equal-length segments and incorporating sequential information during encoding and decoding. Meanwhile, GMIF employs a cross-modality fusion mechanism to effectively fuse the features from the two uncorrelated modalities. Experimental results on the COCO and DIV2K datasets demonstrate that StegaFormer surpasses existing state-of-the-art methods in terms of recovery accuracy, message capacity, and imperceptibility. Our code is released in <https://github.com/boschresearch/Stegaformer>.

1 Introduction

Image steganography is a technique that conceals confidential information within a publicly accessible image [Mielikainen, 2006; Pevný *et al.*, 2010; Zhang *et al.*, 2019a; Tan *et al.*, 2021]. In this study, we focus on message hiding. It has a wide range of applications such as copy-right protection, light field messaging [Wengrowski and Dana, 2019], virtual reality and augmented reality applications [Tancik *et al.*, 2020] and face anonymization [Kishore *et al.*, 2021]. The goal of

it is embedding secret message bits within a cover image to produce a new image (called stego image). Ensuring a balanced trade-off among message capacity, recovery accuracy, and imperceptibility is the task’s core. Generally, message capacity is measured by bits per pixel (BPP). Recovery accuracy indicates the message fidelity after being processed by these methods. Imperceptibility is minimizing the perceptible differences between the cover image and the stego image.

Traditional message hiding methods often rely on heuristic approaches, such as the Least Significant Bit method [Mielikainen, 2006], which modifies individual pixels of a digital image to conceal message bits. Recently, with the advancements of deep learning, latest methods have significantly improved the message capacity and imperceptibility [Zhang *et al.*, 2019a; Yu, 2020; Tan *et al.*, 2021; Wei *et al.*, 2022; Yin *et al.*, 2023]. These methods involve aligning and concatenating message bits with the cover image in a spatial manner while utilizing Convolutional Neural Network (CNN) to seamlessly integrate the message and image.

However, CNN-based approaches often yield suboptimal results in message encoding and recovery, particularly when employing convolutional operations to encode multiple layers of message bits as illustrated in Fig. 1(a). We have identified two main limitations in current CNN-based methods. Firstly, the indiscriminate use of convolutional kernels to encode message bits disrupts the sequential order of the original message bits. Secondly, the element-wise concatenation of message and image features, followed by convolutional operations, underestimates the substantial disparity between these two modalities, resulting in inadequate fusion as shown in Fig. 1(c).

To validate these assumptions, we gradually modified the kernel size of SteganoGAN [Zhang *et al.*, 2019a] and designed experiments at a 4 BPP message capacity using Div2k [Agustsson and Timofte, 2017] dataset. As depicted in Fig. 2, reducing the kernel size enhances the model’s message recovery accuracy. With a decrease in kernel size from 7 to 1, 2D convolution is simplified to linear layer, focusing on 1D message segments along the channel dimension of the message tensor and encoding these segments sequentially. This process maintains the sequential order of the original bit string. On the other hand, the stego image quality improves as the kernel size increases due to a larger receptive field introduces more global interactions between the message and image features.

To address these challenges, as shown in Fig. 1(b), we lever-

*the corresponding author xuchong.qiu@cn.bosch.com

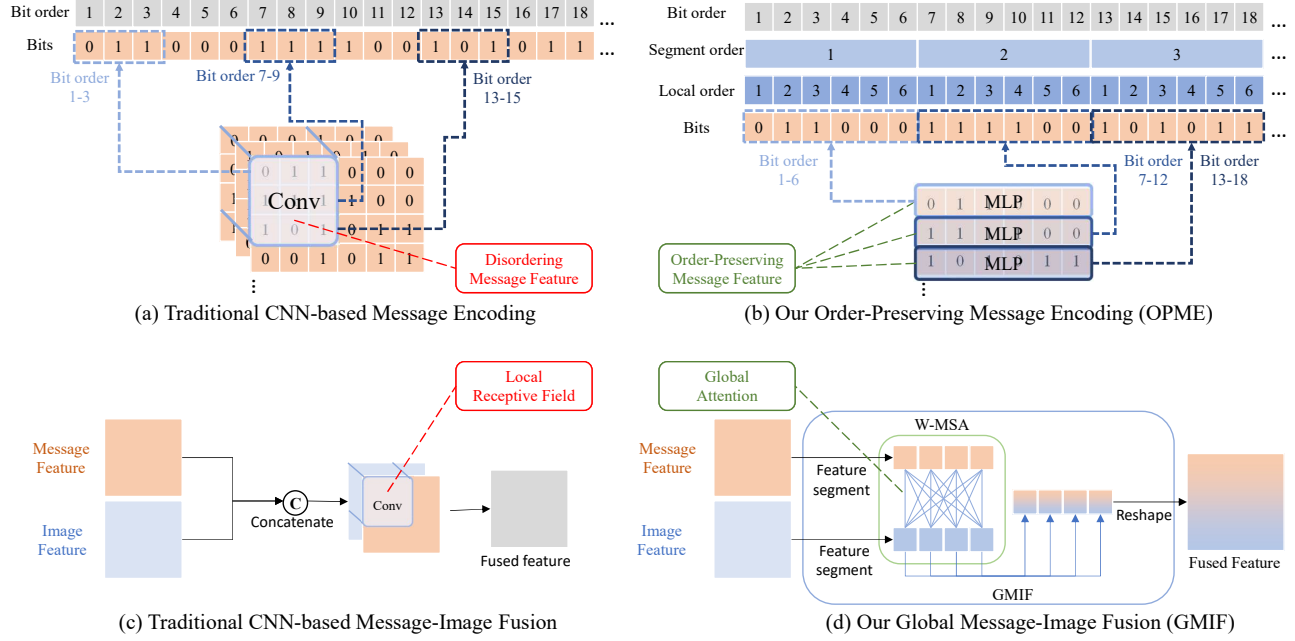


Figure 1: The illustration of our proposed methods. (a) traditional CNN-based message encoding and (b) our proposed MLP-based message encoding: Order-Preserving Message Encoder (OPME) compares the difference in message encoding. (c) traditional feature fusion and (d) our proposed Global Message-Image Fusion (GMIF) is the difference in message-image fusion.

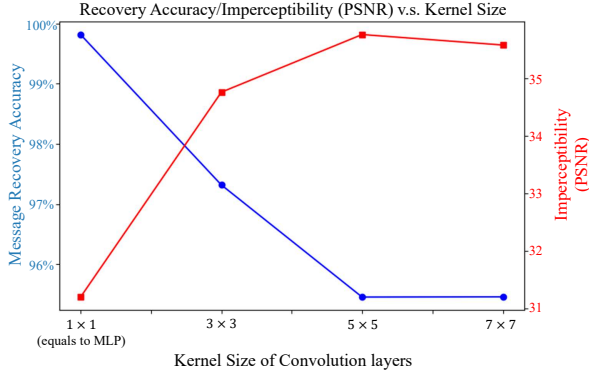


Figure 2: The change in message recovery accuracy and stego image quality was investigated across different kernel sizes using the traditional CNN-based method SteganoGAN. The results reveal that the CNN-based structure struggles to enhance message recovery accuracy while maintaining imperceptibility.

age Multi-Layer Perceptrons (MLP) to design a more appropriate method for message encoding. The MLP-based message encoding phase can focus on small and complete message segments individually. Later, the Multi-Head Self-Attention (MSA) [Vaswani *et al.*, 2017b] and positional embeddings (PEs) help to globally encode the message features while explicitly adding sequential information to the encoded message features. For message and image fusion, as shown in Fig. 1(d), we use Windowed Multi-Head Self-Attention Layer (W-MSA) to address the limitation of receptive fields in the CNN-based structure, enabling global interactions between message and image features.

Our approach, named StegaFormer, consists of three pro-

posed modules for enhanced message encoding, decoding, and message-image fusion, respectively. We design the first two modules, Order-Preserving Message Encoder (OPME) and Order-Preserving Message Decoder (OPMD), to effectively handle message segments while maintaining their order. The OPMD follows the same methodology with OPME to decode the message. Long message bits are segmented into equal-length short messages. Later, MLPs encode and decode them separately [O’shea and Hoydis, 2017]. Additionally, OPME and OPMD take full advantage of sequential order by incorporating PEs into the message features and globally encodes and decodes the features using MSA. The last one, Global Message-Image Fusion (GMIF) employs a W-MSA to fuse the information from the secret message and cover image to the stego image globally, greatly minimizing perceptible artifacts in the stego image.

Comprehensive experiments conducted on real-world datasets demonstrate the superior performance of our model in terms of recovery accuracy, message capacity, and imperceptibility. Importantly, our method exhibits a significant improvement in recovery accuracy. For message capacities ranging from 1 to 4 BPP, StegaFormer maintains a message recovery accuracy exceeding 99%. Even for high-capacity messages, StegaFormer achieves a message recovery accuracy of over 96% at 6 BPP, surpassing the state-of-the-art method that achieves a 3 BPP capacity but with an even lower recovery accuracy. Our contributions are summarized as follows:

- We are the first to point out that CNN disorders message features and is not appropriate for message hiding; consequently, we transfer to an MLP-based approach design.
- We introduce two novel modules OPME & OPMD, which enhance the message encoding and decoding process by

incorporating sequential order into the message.

- We design GMIF, which leverages the global interaction of W-MSA to effectively fuse secret message and cover image features to stego image features.
- Experimental results on real-world datasets demonstrate the remarkable superiority of our framework over existing state-of-the-art methods in terms of accuracy, capacity, and imperceptibility.

2 Related Work

2.1 Message Hiding

Message hiding aims to embed confidential message bits within a cover image, resulting in a stego image, and recover message bits from the stego image. Of course, it also needs to minimize any perceptible differences between cover image and stego image. Thus, the research history is around how to balance the three properties: message capacity, recovery accuracy, and imperceptibility.

Traditional methods often involve altering individual pixels in an image using heuristic techniques. They generally have a high recovery accuracy and imperceptibility, but low capacity. Specifically, early studies [Mielikainen, 2006; Pevný *et al.*, 2010] manipulate the least significant bits of the cover image. Others [Chandramouli *et al.*, 2003; Bi *et al.*, 2007; Reddy and Raja, 2009; Holub and Fridrich, 2012] extend this approach to the frequency domain by transforming the cover image to different types of frequency domains for better performance. Despite their capacity for precise secret message recovery, these methods can only hide an extremely low BPP (*i.e.* 0.4) to evade detection by steganalysis tools [Goljan *et al.*, 2006; Fridrich and Kodovsky, 2012].

Recently, CNN-based methods for message hiding greatly improve capacity and obtain significant attention [Zhang *et al.*, 2019a; Tan *et al.*, 2021; Chen *et al.*, 2022; Yin *et al.*, 2023]. For instances, SteganoGAN [Zhang *et al.*, 2019a] introduces 3D message tensor aligning in the spatial dimensions and ChatGAN [Tan *et al.*, 2021] incorporates channel attention to enhance accuracy and imperceptibility meanwhile keep a high capacity. SFTN [Yin *et al.*, 2023] is proposed to address the rounding error before generating the stego image. However, these CNN-based approaches contribute little to the improvement of message recovery accuracy.

In an effort to address the issue, other works [Kishore *et al.*, 2021; Chen *et al.*, 2023] employ offline optimization, directly optimizing the stego image itself by iteratively adding adversarial perturbations to the stego image rather than improving the message hiding model. While this approach significantly enhances message recovery accuracy, optimizing individual stego images is time-consuming, and imperceptibility is greatly compromised.

Inspired by the difficulties encountered in previous works, we now turn our attention to the details of the message encoding procedure in these CNN-based models. We reveal the main constraint of CNN-based methods: CNNs disorder the message order, thus having limited accuracy. Thus, differing from previous CNN-based methods, we are the first to leverage MLPs with PEs to design an order-preserving framework.

2.2 Multi-head Self-Attention

MSA mechanism is widely adopted in the domain of Natural Language Processing [Vaswani *et al.*, 2017a] and various computer vision tasks [Carion *et al.*, 2020; Zhu *et al.*, 2020; Ranftl *et al.*, 2021; Bai *et al.*, 2022; Li *et al.*, 2022]. The benefits of it stem from the dynamic weights and long-range encoding capability [Khan *et al.*, 2022]. In our approach, we adopt the W-MSA as the fundamental building block of the message-image fusion, enabling long contextual fusion of message and image features with less computational complexity.

3 Methods

As illustrated in Fig. 3, our proposed method encompasses two pipeline for message concealment, *i.e.*, Fig. 3(a), and message recovery, *i.e.*, Fig. 3(b), respectively. This approach sets itself apart from previous works by incorporating three crucial components: the GMIF, as depicted in Fig. 3(c), for the fusion between features from the secret message and cover image, the OPME, as shown in Fig. 3(d), for order-preserving message encoding, OPMD as shown in Fig. 3(e) for corresponding message decoding.

3.1 Preparation

In the message concealment, cover image and secret message are pre-processed before the message-image interaction.

Message Layout Preparation

A secret message $M \in \{0, 1\}^L$, consisting of L bits, is structured in the form $M \in \{0, 1\}^{H \times W \times D}$ in previous approaches [Zhang *et al.*, 2019a; Tan *et al.*, 2021; Chen *et al.*, 2022; Yin *et al.*, 2023]. Here, H and W represent the spatial dimensions of the message tensor, which correspond to the height and width of the cover image, while D denotes the message capacity (*e.g.*, $D = 1$ for 1 BPP message capacity). Although this message layout can be easily processed using convolutional layers, it does introduce inappropriate limitations, as discussed in Sec. 1.

To address the issue, we introduce a unique message layout, where the message $M \in \{0, N_r\}^L$ is reshaped into $M_{\text{seg}} \in \{0, N_r\}^{N_{\text{ms}} \times L_{\text{ms}}}$. Here, N_r denotes the range of message elements (unless explicitly stated otherwise, N_r is set to 1) and N_{ms} represents the number of message segments, L_{ms} represents the length of each message segments, and $L_{\text{ms}} \ll L$. Considering the multi-level structure of StegaFormer, we configure N_{ms} and L_{ms} at different sizes to align with the shape of the corresponding image features.

Image Feature Preparation

Given a cover image $I_{\text{cover}} \in \mathbb{R}^{H \times W \times 3}$, where H and W represent the height and width of the cover image, we employ two stages of operations to extract image feature $F_{\text{im}} \in \mathbb{R}^{(H/2^i \times W/2^i) \times 2^i \times C}$. Here, $i = 1, 2$ indicates the number of stages, and C is the number of channels in the output feature. For models with different message capacities, we set $C = 2 \times L_{\text{ms}}$. Each stage consists of 2D convolution layers followed by a down-sampling operation. The down-sampling operation applies convolution to reduce the spatial size of the feature map by half while doubling its feature

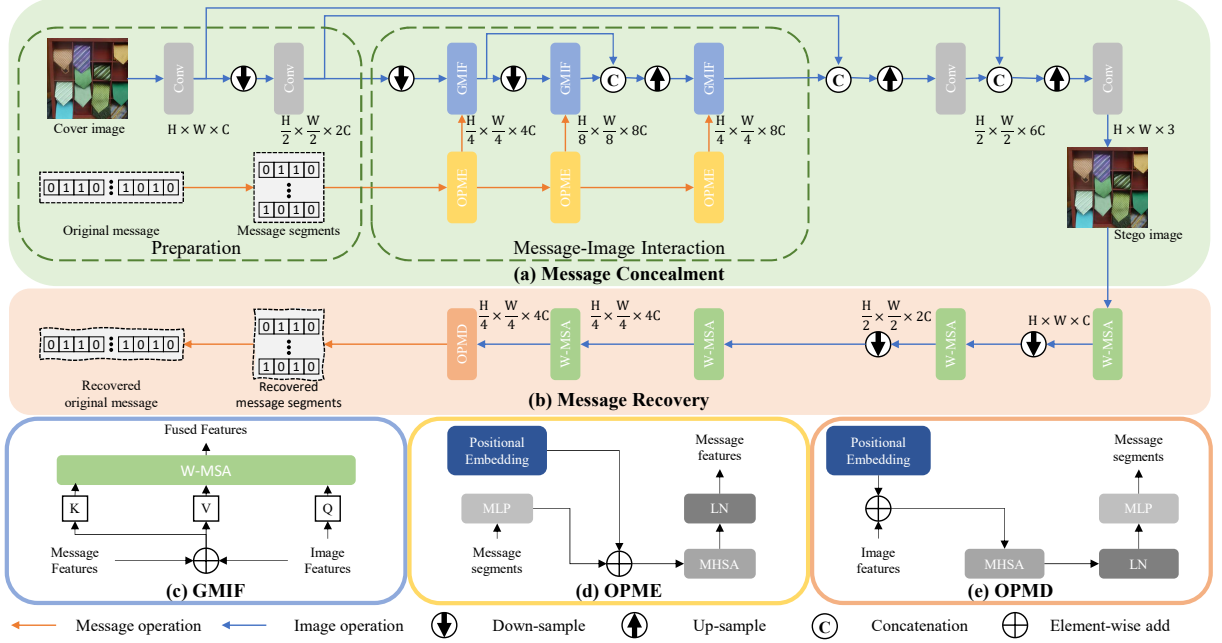


Figure 3: The overview of StegFormer consists of two main pipelines: (a) Message Concealment and (b) Message Recovery, which are facilitated by three proposed components: (c) Global Message-Image Fusion (GMIF), (d) Order-Preserving Message Encoder (OPME), and (e) Order-Preserving Message Decoder (OPMD). The sizes indicated above the modules represent the shapes of their respective outputs. LN denotes Layer Normalization, and W-MSA denotes Windowed Multi-Head Self-Attention Layer.

depth. The output of the image feature preparation phase is $F_{\text{im}} \in \mathbb{R}^{(H/4 \times W/4) \times 4C}$.

3.2 Order-Preserving Modules

Order-Preserving Message Encoder

The main challenge in message encoding lies in effectively converting secret message bits into message features while retaining the sequential information of the message. To address this, we propose an OPME that efficiently encodes the message while preserving both local and global sequential information. In this context, “local” refers to the order within a message segment, while “global” refers to the sequential order of the message segments. Our model consists of three OPME in total to enable multi-scale interaction between the message and image features.

Each OPME incorporates an MLP, referred to as MLP_{enc} , which functions as a channel encoder. Its purpose is to encode message segments $M_{\text{seg}} \in \{0, 1\}^{N_{\text{ms}} \times L_{\text{ms}}}$ into message feature F_{msg} following Eq. (1):

$$F_{\text{msg}} = \text{MLP}_{\text{enc}}(M_{\text{seg}}), \quad (1)$$

where the shape of F_{msg} is equal to the shape of F_{im} at the corresponding GMIF. This learning-based channel encoder [O’shea and Hoydis, 2017] introduces redundancy into the original message segments, facilitating the stable transmission of the message feature within the model.

The importance of maintaining the sequential order of message segments is highlighted by the incorporation of PEs into the encoded segments. This is demonstrated in Eq. (2):

$$F_{\text{msg}}^{\text{global}} = \text{LN}(\text{MHSA}(F_{\text{msg}} + E_{\text{pos}})), \quad (2)$$

where positional embedding E_{pos} is introduced to the F_{msg} followed by a MSA module [Vaswani *et al.*, 2017a] to globally encode F_{msg} to $F_{\text{msg}}^{\text{global}}$. Layer Normalization (LN) [Ba *et al.*, 2016] is employed to normalize the global message features.

Order-Preserving Message Decoder

As depicted in Fig. 3(b), we employ a standard SwinTransformer [Liu *et al.*, 2021] with minor modifications to extract features from I_{stego} . Specifically, the down-sampling operations in the last two layers of the W-MSA module within SwinTransformer are removed to match the spatial size to the feature of the secret message in the OPME. Subsequently, the OPMD reconstructs the secret message segments \hat{M} from the extracted features. The OPMD follows the same methodology as the OPME, but in reverse order.

3.3 Global Message-Image Fusion

Our GMIF, as shown in Eq. (3):

$$F_{\text{stego}} = \text{GMIF}(F_{\text{msg}}^{\text{global}}, F_{\text{im}}), \quad (3)$$

is designed to accomplish two fundamental goals of message hiding. These goals encompass: (1) the stego image should contain all the information from both the secret message and the cover image; (2) the ideal stego image should be identical to the cover image. The key, value and query in the attention mechanism are configured according to these two goals to translate the message and image information to the steganographic features F_{stego} :

$$K = (F_{\text{im}} + F_{\text{msg}}^{\text{global}})W^K, \quad (4)$$

$$V = (F_{\text{im}} + F_{\text{msg}}^{\text{global}})W^V, \quad (5)$$

$$Q = F_{\text{im}}W^Q. \quad (6)$$

Dataset	COCO								
Metric	ACC			PSNR			SSIM		
Capacity	1 BPP	2 BPP	3 BPP	1 BPP	2 BPP	3 BPP	1 BPP	2 BPP	3 BPP
SteganoGAN [Zhang <i>et al.</i> , 2019a]	97.75%	96.46%	91.35%	42.52	39.68	36.45	0.9894	0.9801	0.9650
ChatGAN [Tan <i>et al.</i> , 2021]	99.07%	97.46%	96.18%	46.42	43.17	41.84	0.9943	0.9880	0.9832
StegaFormer (Ours)	99.95%	99.85%	99.68%	47.83	45.30	43.37	0.9969	0.9943	0.9914

Dataset	DIV2K								
Metric	ACC			PSNR			SSIM		
Capacity	1 BPP	2 BPP	3 BPP	1 BPP	2 BPP	3 BPP	1 BPP	2 BPP	3 BPP
SteganoGAN [Zhang <i>et al.</i> , 2019a]	98.96%	97.63%	92.23%	39.36	37.97	36.14	0.9793	0.8916	0.8343
ChatGAN [Tan <i>et al.</i> , 2021]	99.73%	98.63%	94.75%	45.00	42.05	40.63	0.9929	0.9861	0.9782
StegaFormer (Ours)	99.94%	99.87%	99.76%	51.98	49.07	47.31	0.9985	0.9970	0.9958

Table 1: Quantitative comparisons of SteganoGAN, ChatGAN, and our method on the COCO and DIV2K datasets are presented, with the best results highlighted in bold. ACC denotes message recovery accuracy. PSNR and SSIM are two metrics to measure the level of imperceptibility.

The configuration of query, key and value utilized in our approach are inspired by the Transformer-based architecture commonly employed in language translation tasks. Drawing a parallel, we apply a similar mechanism to the task of message hiding sharing, as both involve dealing with a lack of spatial and semantic alignment between the secret message and cover image. The GMIF effectively fuses the optimal stenographic information, which is the sum of $F_{\text{msg}}^{\text{global}}$ and F_{im} , into the desired feature representation of the stego image F_{stego} . Further insights into the various combinations of key, value, and query are provided in the supplementary material.

The basic building block of GMIF is Windowed Multi-Head Self-Attention Layers (W-MSA) [Liu *et al.*, 2021]. One layer of W-MSA with large window size (all window sizes equal to 16) is applied to ensure a comprehensive global interaction between message and image features in the GMIF.

As shown in Eq. (7), we apply up-sampling and convolution layers to the concatenated F_{stego} and F_{im} :

$$I_{\text{res}} = \text{Conv}(\text{Up-Sample}(\text{Concat}(F_{\text{stego}}, F_{\text{im}}))), \quad (7)$$

to reconstruct the residual image I_{res} . The up-sampling layer uses a de-convolution operation to double the height and width of the feature map and reduce the feature dimension by half. The final output of our model is I_{stego} , which is equal to the sum of I_{cover} and I_{res} . Please check supplementary material for more detailed configurations and number of parameters of our model.

3.4 Loss Function

The objectives of message hiding are two-fold: to generate a stego image that closely resembles the cover image and to precisely retrieve the secret message from the stego image. In pursuit of these aims, we employ the loss function as defined in Eq. (8):

$$\mathcal{L}_{\text{total}} = \mathcal{L}_{\text{img}} + \mathcal{L}_{\text{msg}}, \quad (8)$$

$$\mathcal{L}_{\text{img}} = \lambda_1 \mathcal{L}_{\text{MSE}}(I_{\text{cover}}, I_{\text{stego}}) + \lambda_2 \mathcal{L}_{\text{LPIPs}}(I_{\text{cover}}, I_{\text{stego}}), \quad (9)$$

$$\mathcal{L}_{\text{msg}} = \begin{cases} \mathcal{L}_{\text{BCE}}(M, \hat{M}), & \text{if } N_r = 1 \\ \mathcal{L}_{\text{MSE}}(M, \hat{M}), & \text{if } N_r > 1 \end{cases} \quad (10)$$

\mathcal{L}_{img} in Eq. (9) combines a weighted sum of mean square error loss and perceptual loss [Zhang *et al.*, 2018]. We employ

binary cross-entropy loss for \mathcal{L}_{msg} in Eq. (10) when the range of message $N_r = 1$ and \mathcal{L}_{msg} change to mean square error loss when the message range $N_r > 1$.

4 Experiments

To demonstrate the effectiveness of our proposed approach, we conduct a comparative analysis of message recovery accuracy and imperceptibility against two state-of-the-art message hiding methods: SteganoGAN [Zhang *et al.*, 2019a] and ChatGAN [Tan *et al.*, 2021]. This analysis is carried out across different message capacity levels.

Experimental Settings. Following previous studies [Zhang *et al.*, 2019a; Tan *et al.*, 2021], our method is evaluated on two public datasets: COCO [Lin *et al.*, 2014] and DIV2K [Agustsson and Timofte, 2017]. We chose the COCO dataset due to its inclusion of diverse scenes and rich contextual image information, while the DIV2K dataset consists of high-resolution images. The COCO dataset for message hiding contains 25,000 images randomly sampled from the original COCO training split for model training, as well as 500 images randomly sampled from the original COCO test split for model evaluation. The DIV2K dataset contains 800 training images and 100 evaluation images. Throughout both the training and evaluation phases, we fix the image size to 256×256 pixels for both datasets. The training process for each model consists of 100,000 iterations, with a batch size of 2. We set $\lambda_1 = 1 \times 10^{-4}$ and $\lambda_2 = 1 \times 10^{-6}$ to balance these different losses. More detailed configurations of our model are listed in the supplementary material due to the page limitation.

Evaluation Metrics. Three metrics are used to evaluate the model performance. The message recovery accuracy is utilized to assess the percentage of successfully recovered secret messages. The imperceptibility of stego images is measured using the PSNR and SSIM [Wang *et al.*, 2004].

4.1 Comparison with State-of-the-Art Methods

A comprehensive comparison between our method and two existing state-of-the-art methods [Zhang *et al.*, 2019a; Tan *et al.*, 2021] is presented in Tab. 1. Our method consistently outperforms the other methods in terms of recovery accuracy and imperceptibility at 1,2,3 BPP message capacity.

Specifically, at a 3 BPP capacity, our method achieves an impressive recovery accuracy of 99.68% and 99.76% for the COCO and DIV2K datasets, respectively. This represents a significant improvement of 3.5% and 5.0% compared to the current state-of-the-art accuracies achieved by ChatGAN [Tan *et al.*, 2021]. These improvements demonstrate the effectiveness of OPME in achieving high-accuracy message hiding.

Furthermore, our method enhances imperceptibility in terms of both PSNR and SSIM across different message capacities. For example, compared with ChatGAN [Tan *et al.*, 2021] at a 3 BPP message capacity, our method improves the PSNR from 41.84 to 43.37 on the COCO dataset, and from 40.63 to 47.31 on the DIV2K dataset. These results underscore the effectiveness of GMIF in fusion of steganographic information into stego images.

Fig. 4(b) displays residual images generated by our method and previous methods [Zhang *et al.*, 2019a; Tan *et al.*, 2021] at 3 BPP message capacity. Residual images of our method demonstrate that minimal changes have been added to cover images. In contrast, previous approaches spread higher residuals all over the cover image, leading to lower imperceptibility. More qualitative results are in the supplementary material.

4.2 Models for High Message Capacity

BPP	4	6	8
ACC	99.27%	96.65%	91.78%
PSNR	41.87	40.37	34.70
SSIM	0.9877	0.9803	0.9508

Table 2: Quantitative results of StegaFormer with message capacities at 4, 6 and 8 BPP on the COCO dataset.

We conduct a series of experiments to showcase the performance of our method in handling high message capacities. As shown in Tab. 2, the results demonstrate that our method achieves a message recovery accuracy exceeding 90% for message capacities up to 8 BPP. Compared with existing methods, these results highlight the remarkable improvement achieved by our method in both message capacity and recovery accuracy. Besides, Fig. 5(b)(c) depicts the residual and stego images by our models with high message capacities. The residual images of these high-capacity models demonstrate the outstanding imperceptibility of our models.

There are two approaches to increase the message hiding capacity in our method: increasing the length of message segments L_{ms} and expanding the range of message elements N_r . The 4 BPP model has $(L_{ms}, N_r) = (64, 1)$, the 6 BPP model has $(L_{ms}, N_r) = (48, 3)$, and the 8 BPP model has $(L_{ms}, N_r) = (32, 15)$. More details of N_r and L_{ms} are provided in the supplementary material.

4.3 Steganalysis

Steganalysis methods [Boroumand *et al.*, 2018; Zhang *et al.*, 2019b; You *et al.*, 2020] play a crucial role in assessing the security of stego images. Typically, this involves utilizing a machine learning model to classify images as either cover images or stego images. In our study, we choose the state-of-the-art steganalysis approach SiaStegNet [You *et al.*, 2020] to

conduct a comprehensive benchmark comparison between our method and existing methods [Zhang *et al.*, 2019a; Tan *et al.*, 2021]. The SiaStegNet models are trained and evaluated on the COCO dataset.

Fig. 6 presents the steganalysis results, demonstrating that our model achieves the lowest Area Under the Curve (AUC) among the three compared methods. These results indicate that our method exhibits the lowest detection rate and has the best security of stego images. All message hiding models for comparison have a 3 BPP message capacity.

4.4 Ablation Study

To prove the effectiveness of our purposed components. We first evaluate the performance of OPME, OPMD and GMIF. Later, go into the details of the OPME and OPMD.

Effectiveness of OPME, OPMD and GMIF

As illustrated in Tab. 3, to assess the effectiveness of our order-preserving in OPME and OPMD and global interaction design in GMIF, we scale down our model by removing the OPME and OPMD and GMIF step by step to set up a baseline model, then perform the message hiding training at a 4 BPP message payload. In their absence, these components are replaced with 2D convolution layers. It is evident that the absence of both OPME and OPMD and GMIF prevents the model from successfully hiding the secret message within the cover image. A model using only GMIF can boost accuracy via more effective message-image fusion. The involvement of OPME and OPMD significantly increases the accuracy of message recovery, highlighting the effectiveness of preserving message sequential order in message encoding.

Models	ACC	PSNR	SSIM
baseline	50.01%	53.4	0.9988
+GMIF	87.60%	43.78	0.9908
+GMIF+OPME+OPMD	99.24%	41.78	0.9875

Table 3: Ablation of the proposed OPME, OPMD and GMIF. We replace our proposed components with 2D convolution layers in the baseline model which disable the global message-image fusion and the order-preserving message encoding and decoding, respectively.

Effectiveness of PE within OPME and OPMD

MLP	MSA	PE	ACC	PSNR	SSIM
✓	×	×	98.59%	40.59	0.9826
✓	✓	×	98.68%	40.70	0.9833
✓	×	✓	97.92%	40.05	0.9786
✓	✓	✓	99.24%	41.78	0.9875

Table 4: Ablation of the proposed OPME and OPMD. We compare the performance of different version of them, which gradually add the PE and MSA to validate the effectiveness of these components.

As illustrated in Tab. 4, we assess the efficacy of the features of OPME and OPMD at 4 BPP using COCO dataset. We start with the model only contains MLP as a message encoder and decoder. The addition of solely positional embedding or MSA after the MLP module results in sub-optimal performance. The best performance is achieved with the default

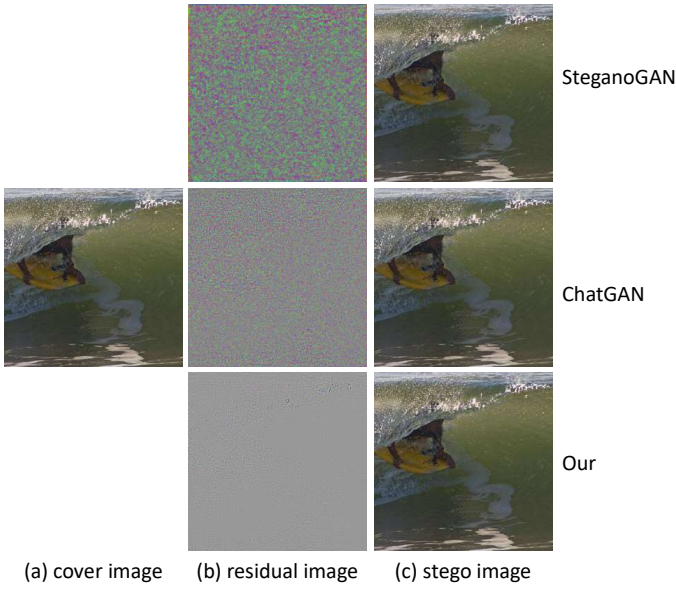


Figure 4: Qualitative results of 3 bits per pixel (BPP) message hiding using different methods: (a) cover image, (b) residual images, and (c) stego images. The images in the top row are obtained from SteganoGAN, those in the middle row from ChatGAN, and the bottom row showcases our method. For enhanced visualization, the residual images are multiplied by 100. Best viewed in digital version.

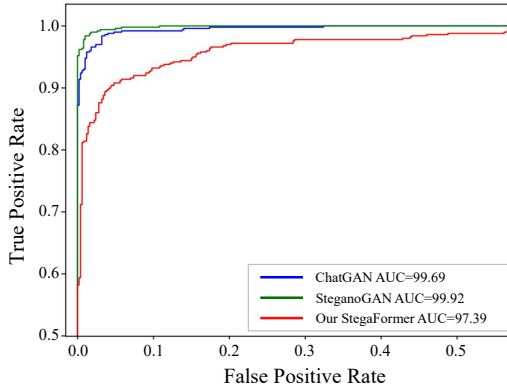


Figure 6: The comparison of the detection accuracy of SiaStegNet models for ChatGAN, SteganoGAN and our approach. Lower AUC represents the stego images by our StegaFormer are more difficult to detect than the other two methods. Our approach shows lowest AUC.

design of our OPME and OPMD, which include MLP, MSA, and PEs.

To further validate whether OPME and OPMD appropriately models the independent nature of message segments, we assess the positional embeddings learned by OPME. More specifically, we compare the characteristics of positional embeddings obtained from ViT with those from OPME. As illustrated in Fig. 7, the positional embeddings obtained from ViT exhibit a prevalence of significant eigenvalues, suggesting that numerous image patches share similar positional information for image classification task. In contrast, the positional embeddings acquired from OPME do not exhibit prominent eigenvalues, indicating that the positional embeddings in OPME contain more independent positional information than those in

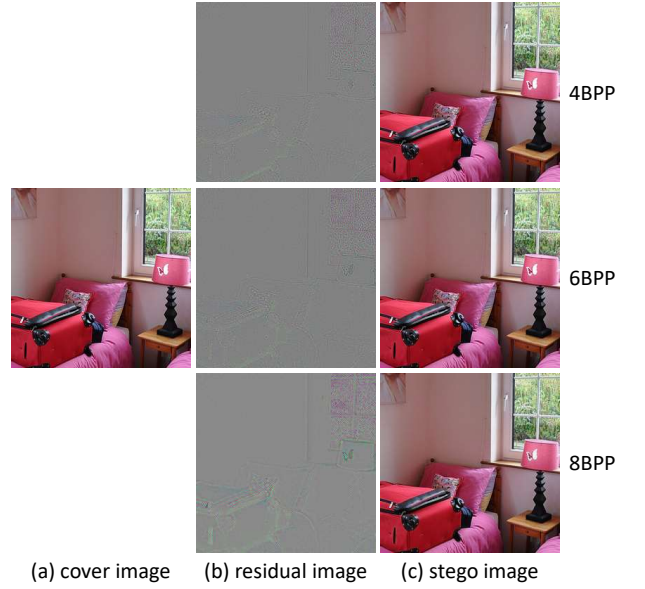


Figure 5: Qualitative results of high-capacity message hiding with our method: (a) cover image, (b) residual images, and (c) stego images. Samples at 4 BPP, 6 BPP, and 8 BPP message capacities are displayed in the first, second, and third rows, respectively. The residual images are multiplied by 100 for visualization. Best viewed in digital version.

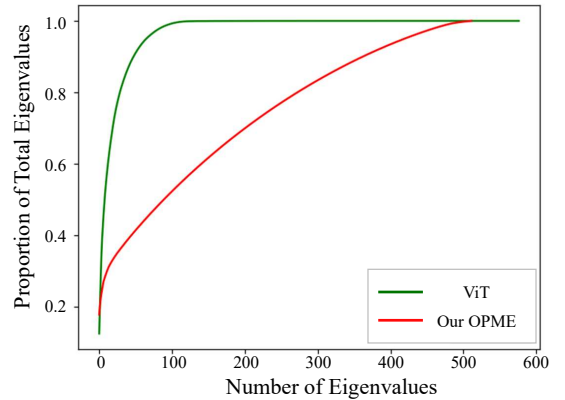


Figure 7: The comparison of the ratio between the cumulative sum of the top n eigenvalues and the sum of all eigenvalues. Green for the PEs from pre-trained ViT and red for the PEs from OPME. The PEs from OPME contain more independent positional information.

ViT. This demonstrates that OPME has effectively learned to assign distinct positional information to each individual message segment.

5 Conclusion

In this paper, we propose StegaFormer, a novel message hiding framework for high accuracy message concealment and recovery. StegaFormer is able to significantly increase the message recovery accuracy by emphasizing the order of message bits and cross-modality feature fusion. Experiments on real-world datasets demonstrate that our method consistently outperforms the state-of-the-art methods in terms of message recovery accuracy, message capacity, and imperceptibility.

Ethical Statement

There are no ethical issues.

Acknowledgments

We thank Wang Wenfeng for conducting early experiments and Lu Lvjian for reviewing the manuscript.

References

- [Agustsson and Timofte, 2017] Eirikur Agustsson and Radu Timofte. Ntire 2017 challenge on single image super-resolution: Dataset and study. In *Proceedings of the IEEE conference on computer vision and pattern recognition workshops*, pages 126–135, 2017.
- [Ba et al., 2016] Jimmy Lei Ba, Jamie Ryan Kiros, and Geoffrey E Hinton. Layer normalization. *arXiv preprint arXiv:1607.06450*, 2016.
- [Bai et al., 2022] Xuyang Bai, Zeyu Hu, Xinge Zhu, Qingqiu Huang, Yilun Chen, Hongbo Fu, and Chiew-Lan Tai. Transfusion: Robust lidar-camera fusion for 3d object detection with transformers. In *Proceedings of the IEEE/CVF conference on computer vision and pattern recognition*, pages 1090–1099, 2022.
- [Bi et al., 2007] Ning Bi, Qiyu Sun, Daren Huang, Zhihua Yang, and Jiwu Huang. Robust image watermarking based on multiband wavelets and empirical mode decomposition. *IEEE Transactions on Image Processing*, 16(8):1956–1966, 2007.
- [Boroumand et al., 2018] Mehdi Boroumand, Mo Chen, and Jessica Fridrich. Deep residual network for steganalysis of digital images. *IEEE Transactions on Information Forensics and Security*, 14(5):1181–1193, 2018.
- [Carion et al., 2020] Nicolas Carion, Francisco Massa, Gabriel Synnaeve, Nicolas Usunier, Alexander Kirillov, and Sergey Zagoruyko. End-to-end object detection with transformers. In *ECCV*, pages 213–229. Springer, 2020.
- [Chandramouli et al., 2003] Rajarathnam Chandramouli, Mehdi Kharrazi, and Nasir Memon. Image steganography and steganalysis: Concepts and practice. In *International Workshop on Digital Watermarking*, pages 35–49. Springer, 2003.
- [Chen et al., 2022] Xiangyu Chen, Varsha Kishore, and Kilian Q Weinberger. Learning iterative neural optimizers for image steganography. In *The Eleventh International Conference on Learning Representations*, 2022.
- [Chen et al., 2023] Xiangyu Chen, Varsha Kishore, and Kilian Q Weinberger. Learning iterative neural optimizers for image steganography. *arXiv preprint arXiv:2303.16206*, 2023.
- [Fridrich and Kodovsky, 2012] Jessica Fridrich and Jan Kodovsky. Rich models for steganalysis of digital images. *IEEE Transactions on Information Forensics and Security*, 7(3):868–882, 2012.
- [Goljan et al., 2006] Miroslav Goljan, Jessica Fridrich, and Taras Holtyak. New blind steganalysis and its implications. In *Security, Steganography, and Watermarking of Multimedia Contents VIII*, volume 6072, page 607201. International Society for Optics and Photonics, 2006.
- [Holub and Fridrich, 2012] Vojtěch Holub and Jessica Fridrich. Designing steganographic distortion using directional filters. In *2012 IEEE International workshop on information forensics and security (WIFS)*, pages 234–239. IEEE, 2012.
- [Khan et al., 2022] Salman Khan, Muzammal Naseer, Munawar Hayat, Syed Waqas Zamir, Fahad Shahbaz Khan, and Mubarak Shah. Transformers in vision: A survey. *ACM computing surveys (CSUR)*, 54(10s):1–41, 2022.
- [Kishore et al., 2021] Varsha Kishore, Xiangyu Chen, Yan Wang, Boyi Li, and Kilian Q Weinberger. Fixed neural network steganography: Train the images, not the network. In *International Conference on Learning Representations*, 2021.
- [Li et al., 2022] Yingwei Li, Adams Wei Yu, Tianjian Meng, Ben Caine, Jiquan Ngiam, Daiyi Peng, Junyang Shen, Yifeng Lu, Denny Zhou, Quoc V Le, et al. Deepfusion: Lidar-camera deep fusion for multi-modal 3d object detection. In *Proceedings of the IEEE/CVF Conference on Computer Vision and Pattern Recognition*, pages 17182–17191, 2022.
- [Lin et al., 2014] Tsung-Yi Lin, Michael Maire, Serge Belongie, James Hays, Pietro Perona, Deva Ramanan, Piotr Dollár, and C Lawrence Zitnick. Microsoft coco: Common objects in context. In *European conference on computer vision*, pages 740–755. Springer, 2014.
- [Liu et al., 2021] Ze Liu, Yutong Lin, Yue Cao, Han Hu, Yixuan Wei, Zheng Zhang, Stephen Lin, and Baining Guo. Swin transformer: Hierarchical vision transformer using shifted windows. In *ICCV*, pages 10012–10022, 2021.
- [Mielikainen, 2006] Jarno Mielikainen. Lsb matching revisited. *IEEE signal processing letters*, 13(5):285–287, 2006.
- [O’shea and Hoydis, 2017] Timothy O’shea and Jakob Hoydis. An introduction to deep learning for the physical layer. *IEEE Transactions on Cognitive Communications and Networking*, 3(4):563–575, 2017.
- [Pevný et al., 2010] Tomáš Pevný, Tomáš Filler, and Patrick Bas. Using high-dimensional image models to perform highly undetectable steganography. In *International Workshop on Information Hiding*, pages 161–177, 2010.
- [Ranftl et al., 2021] René Ranftl, Alexey Bochkovskiy, and Vladlen Koltun. Vision transformers for dense prediction. In *ICCV*, pages 12179–12188, 2021.
- [Reddy and Raja, 2009] HS Manjunatha Reddy and KB Raja. High capacity and security steganography using discrete wavelet transform. *International Journal of Computer Science and Security (IJCSS)*, 3(6):462, 2009.
- [Tan et al., 2021] Jingxuan Tan, Xin Liao, Jiate Liu, Yun Cao, and Hongbo Jiang. Channel attention image steganography

- with generative adversarial networks. *IEEE Transactions on Network Science and Engineering*, 2021.
- [Tancik *et al.*, 2020] Matthew Tancik, Ben Mildenhall, and Ren Ng. Stegastamp: Invisible hyperlinks in physical photographs. In *CVPR*, 2020.
- [Vaswani *et al.*, 2017a] Ashish Vaswani, Noam Shazeer, Niki Parmar, Jakob Uszkoreit, Llion Jones, Aidan N Gomez, Łukasz Kaiser, and Illia Polosukhin. Attention is all you need. In *Advances in Neural Information Processing Systems*, volume 30, 2017.
- [Vaswani *et al.*, 2017b] Ashish Vaswani, Noam Shazeer, Niki Parmar, Jakob Uszkoreit, Llion Jones, Aidan N Gomez, Łukasz Kaiser, and Illia Polosukhin. Attention is all you need. *Advances in neural information processing systems*, 30, 2017.
- [Wang *et al.*, 2004] Zhou Wang, Alan C Bovik, Hamid R Sheikh, and Eero P Simoncelli. Image quality assessment: from error visibility to structural similarity. *IEEE transactions on image processing*, 13(4):600–612, 2004.
- [Wei *et al.*, 2022] Ping Wei, Sheng Li, Xinpeng Zhang, Ge Luo, Zhenxing Qian, and Qing Zhou. Generative steganography network. In *Proceedings of the 30th ACM International Conference on Multimedia*, pages 1621–1629, 2022.
- [Wengrowski and Dana, 2019] Eric Wengrowski and Kristin Dana. Light field messaging with deep photographic steganography. In *CVPR*, 2019.
- [Yin *et al.*, 2023] Xiaolin Yin, Shaowu Wu, Ke Wang, Wei Lu, Yicong Zhou, and Jiwu Huang. Anti-rounding image steganography with separable fine-tuned network. *IEEE Transactions on Circuits and Systems for Video Technology*, 2023.
- [You *et al.*, 2020] Weike You, Hong Zhang, and Xianfeng Zhao. A siamese cnn for image steganalysis. *IEEE Transactions on Information Forensics and Security*, 16:291–306, 2020.
- [Yu, 2020] Chong Yu. Attention based data hiding with generative adversarial networks. In *Proceedings of the AAAI conference on artificial intelligence*, volume 34, pages 1120–1128, 2020.
- [Zhang *et al.*, 2018] Richard Zhang, Phillip Isola, Alexei A Efros, Eli Shechtman, and Oliver Wang. The unreasonable effectiveness of deep features as a perceptual metric. In *CVPR*, pages 586–595, 2018.
- [Zhang *et al.*, 2019a] Kevin Alex Zhang, Alfredo Cuesta-Infante, and Kalyan Veeramachaneni. Steganogan: High capacity image steganography with gans. *arXiv preprint arXiv:1901.03892*, 2019.
- [Zhang *et al.*, 2019b] Ru Zhang, Feng Zhu, Jianyi Liu, and Gongshen Liu. Depth-wise separable convolutions and multi-level pooling for an efficient spatial cnn-based steganalysis. *IEEE Transactions on Information Forensics and Security*, 15:1138–1150, 2019.
- [Zhu *et al.*, 2020] Xizhou Zhu, Weijie Su, Lewei Lu, Bin Li, Xiaogang Wang, and Jifeng Dai. Deformable detr: Deformable transformers for end-to-end object detection. In *International Conference on Learning Representations*, 2020.